



HAL
open science

Early Systemic Bacterial Dissemination and a Rapid Innate Immune Response Characterize Genetic Resistance to Plague of SEG Mice

Christian E. Demeure, Charlène Blanchet, Catherine Fitting, Corinne Fayolle, Huot Khun, Marek Szatanik, Geneviève Milon, Jean-Jacques Panthier, Jean Jaubert, Xavier Montagutelli, et al.

► To cite this version:

Christian E. Demeure, Charlène Blanchet, Catherine Fitting, Corinne Fayolle, Huot Khun, et al.. Early Systemic Bacterial Dissemination and a Rapid Innate Immune Response Characterize Genetic Resistance to Plague of SEG Mice. *Journal of Infectious Diseases*, 2012, 205 (1), pp.134-143. 10.1093/infdis/jir696 . pasteur-02073619

HAL Id: pasteur-02073619

<https://pasteur.hal.science/pasteur-02073619>

Submitted on 20 Mar 2019

HAL is a multi-disciplinary open access archive for the deposit and dissemination of scientific research documents, whether they are published or not. The documents may come from teaching and research institutions in France or abroad, or from public or private research centers.

L'archive ouverte pluridisciplinaire **HAL**, est destinée au dépôt et à la diffusion de documents scientifiques de niveau recherche, publiés ou non, émanant des établissements d'enseignement et de recherche français ou étrangers, des laboratoires publics ou privés.



Distributed under a Creative Commons Attribution - NonCommercial - ShareAlike 4.0 International License

1 Early systemic bacterial dissemination and a rapid innate immune
2 response characterize genetic resistance to plague of SEG mice

3

4 Christian E. Demeure¹, Charlène Blanchet², Catherine Fitting³, Corinne Fayolle¹, Huot Khun⁴,
5 Marek Szatanik², Geneviève Milon⁵, Jean-Jacques Panthier², Jean Jaubert², Xavier Montagutelli²,
6 Michel Huerre⁴, Jean-Marc Cavaillon³, and Elisabeth Carniel¹

7

8 ¹*Yersinia* Research Unit

9 ²Mouse Functional Genetics Unit

10 ³Unité Cytokines et Inflammation

11 ⁴Unité de recherche et d'expertise Histotechnologie et Pathologie

12 ⁵Unité Immunophysiologie et Parasitisme Intracellulaire,

13 Institut Pasteur, 75724 Paris, France.

14

15

16 Abstract : 199 words

17 Text: 3473 words

18

19 Running Title: Innate immunity in plague resistant mice

20

21 **Footnotes**

22

23 Potential conflict of interest: none.

24

25 Financial support: This study was supported by a BIOTOX grant from the French Ministry of
26 Health and a grant from Aventis Pharma (Sanofi-Aventis group) and Bayer Pharma as part of a
27 multi-organism call for proposal. CB is a recipient of a DGA (*Délégation Générale pour*
28 *l'Armement*) fellowship. The Mouse functional Genetics Unit was supported by Merck Serono.

29

30 Preliminary results of this work were presented by E. Carniel at the “9th International Symposium
31 on Yersinia” (Oct. 10-14th, 2006) in Lexington, Kentucky.

32

33 New affiliations:

34 M. Szatanik: “Unité Postulante Infections Bactériennes Invasives“, Institut Pasteur, 75724 Paris,
35 France.

36 C. Blanchet: “Unité Cytokines et Inflammation“, Institut Pasteur, 75724 Paris, France.

37 Corinne Fayolle: “Service de l’Enseignement“, Institut Pasteur, 75724 Paris, France.

38

39 Reprints or correspondence: C.E. Demeure, *Yersinia* Research Unit, Institut Pasteur, 28 rue du Dr
40 Roux, Paris 75724, France. E-mail: cdemeure@pasteur.fr, Tel: 33-1-45688448, Fax: 33-1-
41 45688954

42

43 **Abstract**

44

45 **Background:** While laboratory mice are usually highly susceptible to *Yersinia pestis*, we
46 recently identified a mouse strain (SEG) that exhibited an exceptional capacity to resist bubonic
47 plague and used it to identify immune mechanisms associated with resistance.

48 **Methods:** The kinetics of infection, circulating blood cells, granulopoiesis, lesions and cellular
49 populations in the spleen, and cytokine production in various tissues were compared in SEG and
50 susceptible C57BL/6J mice after subcutaneous infection with the virulent *Y. pestis* CO92.

51 **Results:** Strikingly, bacterial invasion occurred early (day 2) but was transient in SEG/Pas,
52 while in C57BL/6J it was delayed but continuous until death. The bacterial load in all organs
53 significantly correlated with the production of five cytokines (G-CSF, KC, MCP-1, IL-1 α and IL-
54 6) involved in monocyte and neutrophil recruitment. Indeed, higher proportions of these two cell
55 types in blood and massive recruitment of F4/80+CD11b- macrophages in spleen were observed in
56 SEG/Pas at early time point (day 2). Later times post-infection (day 4) were characterized in
57 C57BL/6J by destructive lesions of the spleen and impaired granulopoiesis.

58 **Conclusion:** A fast and efficient *Y. pestis* dissemination in SEG may be critical for the triggering
59 of an early and effective innate immune response necessary for surviving plague.

60

61 **Keywords:** *Yersinia pestis*, plague, *Mus spretus*, *Mus musculus*, dissemination, F4/80+
62 macrophages, Polymorphonuclear neutrophils.

63

64 INTRODUCTION

65 Plague has caused three pandemics that killed 200 millions of human beings [1, 2]. Despite
66 considerable progresses in its prevention and cure, the disease persists today on three continents
67 (Africa, Asia and America) [3] and has resurged in areas considered plague-free for several
68 decades, leading to its categorization as a re-emerging disease [4]. This threat has been further
69 exacerbated by the isolation of *Yersinia pestis* strains naturally resistant to antibiotics [5, 6], and by
70 their potential use for bioterrorism.

71 Bubonic plague, the most common clinical presentation, results from the bite of infected fleas.
72 After intradermal penetration, *Y. pestis* disseminates via lymphatic vessels to draining lymph nodes
73 and then spread to various tissues (spleen, liver) before causing a fatal septicemia [7, 8]. Without
74 prompt diagnosis and antibiotherapy, bubonic plague is rapidly lethal in 50-70% of cases [1].
75 Strikingly, little is known about the characteristics of the systemic and local host responses
76 specifically targeted by *Y. pestis* during the infectious process.

77 During Middle Ages, some individuals were able to survive bubonic plague, suggesting a
78 genetic determinism of resistance. Non-human mammalian species display variable levels of
79 susceptibility to plague [1]. The host mechanisms responsible for these different responses are
80 unknown but are most likely genetically determined. Even rodents, the major plague reservoir,
81 display a wide susceptibility spectrum. The observation that the progeny of various rodent species
82 trapped in plague foci is significantly more resistant to plague than their counterparts from non-
83 plague foci [9-12], suggests the selection of protective allelic combinations under *Y. pestis*
84 pressure.

85 Laboratory mice (*Mus musculus*), a widely used experimental model to study *Y. pestis*
86 pathophysiology, are usually highly susceptible to plague (*Y. pestis* 50% lethal dose (LD₅₀) of ≈10
87 cfu upon subcutaneous (sc) infection) [13]. However, mice resisting an intravenous (iv) inoculation
88 of high doses of *Y. pestis* KIM5 were recently reported [14, 15]. Genetic studies subsequently

89 showed that their resistance was at least in part associated with ≥ 30 cM of 129-derived genomic
90 DNA near the *III0* locus [16], or with the Major Histocompatibility Complex region on
91 chromosome 17 [15]. Some resistant strains (129 substrain) displayed an acute inflammatory
92 cellular response [17], and others (BALB/cJ) a lower production of IL-6 [15]. Although these
93 studies brought valuable new information about genetic determinants and physiological
94 mechanisms of resistance to plague, their drawback is that they used an attenuated *Y. pestis* KIM5
95 strain (deleted of the High-Pathogenicity Island) that had to be injected by a non-physiological
96 route (iv). Actually, the 129 mice were as susceptible as other laboratory mice when a fully virulent
97 *Y. pestis* was injected sc [17].

98 We recently showed that the SEG/Pas (SEG) mouse strain exhibits high resistance to a sc
99 infection with a fully virulent *Y. pestis* [18]. This mouse strain (*Mus spretus*) is derived from wild
100 progenitors and has been established as an inbred strain [19]. While 100 cfu killed 94% of the
101 C57BL/6J animals (B6), only 10% of SEG mice succumbed. Furthermore, the LD₅₀ of *Y. pestis* for
102 B6 was 3.2 cfu, whereas that for SEG was $>10^7$ cfu [18]. The availability of this mouse strain
103 provided a unique opportunity to identify pathophysiological mechanisms of resistance to plague,
104 by comparing the infectious process and the host response in susceptible (B6) and resistant (SEG)
105 animals.

106

107

108 **MATERIALS AND METHODS**

109

110 **Bacterial growth conditions.**

111 *Y. pestis* CO92 was grown in Luria-Bertani (LB) broth or on LB agar supplemented with 0.2%
112 hemin for 48h at 28°C, in a BSL3 laboratory. Kinetics of bacterial growth in mouse serum were
113 determined by inoculating 10^3 cfu/ml of CO92 grown at 37°C in undecomplemented pooled sera

114 from 7 mice. The sera were incubated at 37°C for 48h and aliquots were taken at various intervals,
115 diluted and plated on LB-H.

116

117 **Mouse experiments**

118 Infection with *Y. pestis* was performed in a BSL3 animal facility, according to the Institut Pasteur
119 guidelines. Groups of 8-12 weeks old female C57BL/6J (Charles River) or SEG/Pas (Institut
120 Pasteur) received a sc injection of 100 cfu in the abdominal skin. Mortality was followed for 14
121 days. To study bacterial spread and host responses, groups of five mice were sacrificed on D1-4
122 post-infection (pi), and their blood, spleen, liver (one lobe), lungs, inguinal lymph nodes and
123 femurs were collected. One half of the spleen and liver was fixed for immunohistological analyses,
124 while the other half, the lungs and inguinal lymph nodes were homogenized using glass beads
125 (VWR) to evaluate bacterial load. The remaining of supernatants of grinded organs and serum were
126 sterile-filtered and frozen for cytokine measurement. Blood formula was determined using a
127 Vet'ABC counter (SCIL).

128

129 **Immunohistological analyses**

130 Organs fixed with 4% paraformaldehyde were dehydrated and embedded in paraffin. Five
131 micrometer sections were stained with hematoxylin and eosin. PMNs were quantified
132 microscopically using a score ranging from 0 (normal) to 5 (large areas filled with infiltrating
133 PMNs) and hemorrhages were scored from 0 (normal) to 3 (extended hemorrhages) on at least
134 three complete sections per sample. For immunohistological labeling of bacteria, sections were
135 incubated with a *Y. pestis* F1-specific rabbit antiserum (Institut Pasteur) followed by Rabbit
136 specific Histofine® MAX-PO (Nichirei). Peroxidase was detected using the AEC substrate
137 (Sigma) with hematoxylin counterstaining.

138

139 **Cytokine/chemokine assays**

140 Measurement of IL-1 α , IL-1 β , IL-10, TNF α , INF γ , IL-6, IL-12p70, G-CSF, KC, and MCP-1 was
141 performed with the BioPlex cytokine bead array (Bio-Rad), using a Luminex platform.

142

143 **Flow cytometry analyses**

144 Minced bone marrow and spleen tissues were passed through a 70 μ m mesh (BD biosciences), and
145 red cells were lysed using Gey's method [20]. Polymorphonuclear neutrophils (PMN:
146 CD11b+Ly6G^{hi}SSC^{hi}), T cells (TCR+), bone marrow monocytes (CD11b+Ly6G-SSC^{int}), spleen
147 red pulp macrophages (F4/80+CD11b-Ly6G-) and other macrophages (CD11b+F4/80-Ly6G-)
148 were quantified using specific fluorescent antibodies: anti-CD11b-Pacific Blue (eBiosciences),
149 anti-TCRbeta-Alexa488, anti-F4/80-Allophycocyanin (Invitrogen), and anti-Ly6G-PE mAb clone
150 1A8 (BD Biosciences). Cells were analyzed with a CyAn cytometer (Beckman-Coulter).

151

152 **Statistical analyses**

153 Statistical analyses included the Mann-Whitney-Wilcoxon test (quantitative parameters), Spearman
154 test (cfu and cytokine contents), and Fisher exact test (mortality).

155

156 **RESULTS**

157

158 **Mouse infections**

159 To compare the progression of the infection and the host response in susceptible and resistant mice,
160 29 SEG and 30 B6 animals were infected sc with 100 cfu of *Y. pestis* CO92. A group of 9-10
161 animals was kept to follow mortality over 14 days (mortality group), and the 20 remaining mice
162 (study group) were distributed in four cages to be analyzed on D1 to D4 pi. Ascribing *a priori* a
163 day of sacrifice to each group prevented the bias of selecting in the latest days the animals that
164 better resisted the infection in the early phase.

165 In the mortality group, B6 started to develop clinical symptoms of infection and to die on D3 pi,
166 and 18/20 were dead on D14. In contrast, SEG developed clinical signs of disease such as
167 prostration and ruffled fur earlier (D2), but started to recover on D4, and 17/19 animals survived
168 and looked healthy on D14. The difference in survival was highly significant ($p < 0.0001$). Body
169 weight variations correlated with symptoms. Body weight loss in B6 mice began on D3 and
170 reached 10% on D4, while body weight of SEG mice remained constant (Supplementary Figure
171 1A).

172 In the study group, one B6 mouse died on D4, and therefore only 9 animals were available for
173 study at this time point.

174

175

176 **Comparison of the infectious process in SEG and B6**

177 Bacterial loads in SEG and B6 followed clearly distinct kinetics over the four days study period. A
178 few circulating *Y. pestis* cells were detected in the blood of both mouse strains on D1, but they
179 reached much higher numbers in the blood of SEG on D2 (Figure 1A). However, bacteremia
180 subsequently decreased in SEG while it increased in B6, so that similar cfu numbers were found on
181 D3 in the blood of the two mouse strains. On D4, SEG had cleared circulating bacteria while the
182 bacterial load had continued to rise in B6.

183 Remarkably, a similar higher bacterial load was observed in all collected organs of SEG
184 (although statistically significant in the lungs only) on D2 (Figure 1 B-E). The bacterial loads then
185 stabilized and started to decline in most SEG organs. In contrast *Y. pestis* numbers rose
186 continuously in B6 tissues, so that much higher bacterial loads were found in all B6 tissues
187 analyzed (except lungs) on D4. The kinetics of infection was highly reproducible for the two
188 groups of mice during two independent experiments.

189 Therefore, both susceptible and resistant mice were efficiently colonized by *Y. pestis*, but SEG
190 displayed an earlier bacterial invasion that was transient.

191

192 *Y. pestis* growth in serum of SEG and B6

193 Since one of the most remarkable differences between resistant and susceptible animals was the
194 capacity of SEG to clear circulating bacteria, we questioned whether a bactericidal component with
195 a higher activity or in greater amount could be present at homeostasis or produced during infection
196 in the serum of resistant mice. The growth curves of *Y. pestis* were similar in the
197 undecomplemented sera of the two mouse strains, before and two days post-infection
198 (Supplementary Figure 1B), indicating that SEG resistance is not attributable to the presence or
199 release of a circulating antibacterial compound.

200

201 SEG and B6 blood cell populations during the infectious process

202 As bacterial clearance from the blood stream may also result from a cell-mediated process, the
203 circulating cell populations during the course of infection were analyzed in SEG and B6. A
204 significant increase in blood leukocyte numbers was observed between D0 and D1 in both mouse
205 strains ($p < 0.02$). However, leukocytosis persisted in SEG but not in B6, so that a marked difference
206 in blood leukocytes was observed on D4 (Figure 2Aa). The same trend was noted for platelets
207 (Figure 2Ab), while erythrocyte counts remained stable (Figure 2Ac), showing the specific increase
208 of some blood cell populations in SEG. Within the leukocyte populations, lymphocytes, monocytes
209 and polymorphonuclear cells (PMN) numbers rose in the two mouse strains on D1-2 pi (Figure
210 2Ad-f). PMNs and monocytes (but not lymphocytes) continued to increase over the study period,
211 moderately in B6 and much more significantly in SEG.

212 Since the marked difference in circulating PMN and monocytes on D4 could result from a more
213 efficient hematopoiesis in SEG, we examined the bone marrow cell populations in the two mouse
214 strains. Before infection, the total cell content in the femurs was significantly higher in B6
215 ($31 \pm 0.4 \times 10^6$) than in SEG ($21 \pm 1.9 \times 10^6$), probably because of the larger body size of B6 (19.8 ± 0.6
216 g) than SEG (16.6 ± 1.6 g). The percentages of PMNs and monocytes in the bone marrow were

217 nonetheless similar in the two species, but became significantly higher in SEG on D4 (Figure 2B),
218 suggesting a more efficient bone marrow hematopoiesis at a late stage of infection in resistant
219 mice.

220

221 **Tissue lesions in infected B6 and SEG**

222 The liver of the two mouse strains exhibited similar histological lesions (mild inflammation with
223 occasional weak hemorrhages and PMN infiltrates), which were moderate at all time points (data
224 not shown). In contrast, tissue lesions characterized by a mild inflammatory infiltrate primarily
225 composed of PMNs were observed in the spleen of B6 and SEG on D1-2, and subsequently became
226 more pronounced in B6 (Figure 3A). Hemorrhages appearing on D2 and increasing over time were
227 always more important in B6 spleens. At late time points (D4), B6 spleens exhibited necrotic
228 lesions destroying the red pulp (Figure 3Ba) and containing free bacteria (Figure 3Bc). In contrast,
229 microabscesses appearing as rare and well contained round foci of PMN infiltration without
230 necrosis started to develop on D4 in SEG spleens (Figure 3Bb), and bacteria were mostly found
231 within these microabscesses (Figure 3Bd). The infectious course in SEG thus differs from that of
232 B6 by less destructive lesions of the spleen and the capacity to circumscribe bacterial foci.

233

234 **Spleen cell populations in uninfected or infected B6 and SEG mice**

235 To further investigate the differences in spleen responses, groups of 6-7 B6 and SEG mice were
236 sacrificed before infection or on D2 pi, and their spleen cell populations were analyzed. The
237 experiments were done twice and the results were pooled.

238 In non-infected animals, total spleen cells were in higher numbers in B6, as expected from their
239 larger spleen size (31±18 mg in B6 versus 16±4 mg in SEG). Both mouse strains had similar
240 proportions of F4/80± CD11b+ macrophages and undetectable PMN (CD11b+ Ly6G+) levels
241 (Figure 3C, diamonds). The main difference was a higher percentage of T cells in B6 and of
242 F4/80+ CD11b- macrophages in SEG.

243 After two days of infection, total splenocytes increased in the two mouse groups, indicating an
244 early cell recruitment (Figure 3C, circles). The drop in T lymphocytes percentages in both mouse
245 groups demonstrated that this cell enrichment was not due to an adaptive response. The proportion
246 of CD11b⁺ macrophages was not significantly affected by the infection. In agreement with our
247 histological observations, the moderate recruitment of PMNs (\approx 1.5% of spleen cells) observed in
248 the two mouse strains could not account for the increased spleen cellularity on D2. The major
249 change in both infected mouse strains was a significant increase in the F4/80⁺ CD11b⁻ macrophage
250 population, which was considerably higher in SEG. Actually, this cell type represented 40% of the
251 splenocytes in infected SEG spleen versus \approx 15% in B6. Immunohistolabeling of the F4/80 antigen
252 in spleen sections indicated that all F4/80⁺ macrophages were located in the red pulp (data not
253 shown).

254 Therefore, SEG have a higher basal level of F4/80⁺ red pulp macrophages and they show a
255 remarkable expansion during infection.

256

257 **Kinetics of cytokine release in the blood and organs of SEG and B6**

258 The production of ten cytokines known to participate to the innate immune response was quantified
259 in the plasma, lymph nodes and spleen of SEG and B6 during the course of infection. Five
260 cytokines (IFN γ , TNF α , IL-1 β , IL-10 and IL-12p70) exhibited similar levels of production in the
261 two mouse strains during the infectious process, despite higher levels of four of them in B6 plasma
262 prior to infection (Supplementary Figure S2).

263 The other five cytokines (G-CSF, KC, MCP-1, IL-1 α and IL-6) displayed a clearly different
264 kinetics of production in the two mouse strains (Figure 4). Most remarkably, their levels were
265 correlated in the three biological samples tested. The pattern in SEG was characterized by a peak of
266 production in the plasma and lymph nodes on D2, and in the spleen on D3. The levels of these
267 cytokines were significantly lower in the organs of B6 at the same time points. At a later stage of
268 infection (D4), the amounts of these five cytokines started to decline in SEG organs, while they

269 continued to rise or remained high (MCP-1) in B6, so that higher levels were detected in the plasma
270 and lymph nodes of B6 on D4.

271 Therefore, *Y. pestis* infection in resistant mice was characterized by a faster but transient
272 production of G-CSF, KC, MCP-1, IL-1 α and IL-6, while susceptible mice displayed a delayed but
273 continuously increasing cytokine response.

274

275 **Correlation between cytokine release and bacterial load in SEG and B6**

276 Interestingly, the kinetics of production of these five cytokines in SEG and B6 seemed to parallel
277 the bacterial loads observed in the two mouse strains. Since cfu and cytokine data were available
278 for each individual animal, the association between the bacterial burden in the plasma, spleen and
279 lymph nodes (whatever the infection day) and the release of the ten cytokines studied was
280 investigated.

281 The levels of the five cytokines that were not differentially produced between B6 and SEG
282 (IFN γ , TNF α , IL-1 β , IL-10 and IL-12p70) were most often not correlated with bacterial loads
283 (Table 1). In contrast, a remarkable and significant correlation was observed between the levels of
284 G-CSF, KC, MCP-1, IL-1 α and IL-6 and the number of bacteria present in most mouse organs
285 (Table 1). This correlation was true for both SEG and B6.

286 Our results thus indicate that, even if the kinetics of production of these five cytokines differed
287 between susceptible and resistant mice, both mouse strains have the capacity to develop the same
288 cytokine response when exposed to similar bacterial loads.

289

290 **DISCUSSION**

291

292 The wild-derived SEG mouse strain naturally exhibits an exceptional capacity to resist an
293 otherwise lethal subcutaneous infection with *Y. pestis* [18]. We took advantage of this

294 unprecedented ability to survive bubonic plague to study pathophysiological mechanisms and host
295 responses associated with the resistance phenotype. To do so, the course of infection and innate
296 immune response were compared in resistant SEG and susceptible B6 mouse strains. The most
297 remarkable and unexpected feature that emerged from this comparison was that *Y. pestis* colonized
298 rapidly and more efficiently the organs of resistant mice. This was evidenced by clinical symptoms
299 of infection that appeared on D2 in SEG, and were retarded (D4) in B6.

300 The higher bacterial load in SEG on D2 was accompanied by a higher in situ production of five
301 cytokines (G-CSF, KC, MCP-1, IL-1 α and IL-6). This rapid cytokine release is most likely the
302 direct consequence of the bacterial burden since we found a highly significant correlation between
303 the number of cfu and cytokine levels in each organ of each individual mouse tested. Of note, this
304 correlation was not observed for the other five cytokines analyzed (IFN γ , TNF α , IL-1 β , IL-10 and
305 IL-12p70). A characteristic of the former group is that, in addition to being produced by bone
306 marrow derived cells, they all are also released by somatic cells such as endothelial cells,
307 fibroblasts and keratinocytes. This points at stromal cells rather than immune cells as a potential
308 source for the early and coordinate production of G-CSF, KC, MCP-1, IL-1 α and IL-6 upon
309 stimulation by *Y. pestis*.

310 This early release may explain the higher numbers of circulating blood monocytes and PMN in
311 SEG on D2. Indeed, MCP-1 is one of the key chemokines that regulate migration and infiltration of
312 monocytes/macrophages at inflammatory sites [21, 22]. G-CSF and IL-6 induce granulocyte
313 mobilization from the bone marrow and their activation, differentiation, and survival [23-25], and
314 KC and IL-1 α promote their chemotaxis [26, 27]. Since neutrophils and monocytes are key
315 components of the host innate response to many bacterial pathogens [28-30], they most likely
316 participate actively to *Y. pestis* clearance from the blood of SEG.

317 The early time points of infection in SEG were also characterized by a massive and specific
318 expansion of F4/80+ CD11b- macrophages in the spleen, an organ important for capturing
319 circulating bacteria. F4/80+ CD11b- macrophages reside in the liver (Kupffer cells) and the spleen,

320 in which they are restricted to the red pulp. Therefore, in contrast to CD11b⁺ macrophages, they
321 are not in contact with lymphocytes and thus are not key players of the adaptive immunity. They
322 are rather effectors of the innate response by phagocytosing blood bacteria penetrating into the
323 highly vascularized red pulp of the spleen and by producing microbicidal metabolites [31]. F4/80⁺
324 CD11b⁻ macrophages may thus be critical for the ability of SEG to respond rapidly and efficiently
325 to a *Y. pestis* infection. An afflux of spleen macrophages was not observed in resistant 129 mice
326 [17], indicating a distinct innate response in these mice. It is worth noting that the proportion of this
327 subpopulation was already higher in SEG than B6 prior to infection, suggesting that SEG are
328 already 'pre-programmed' to mount a more efficient F4/80⁺ CD11b⁻ mediated cellular response.

329 D2 appears as a critical time point at which the host response is already committed to resistance
330 or susceptibility. The differences observed later during infection (D3-4) may therefore simply
331 reflect the consequences of an engagement of the host response towards bacterial clearance or
332 multiplication. Indeed, later time points showed the containment and progressive decrease of the
333 bacterial load in SEG (with a complete recovery of most animals), and a continuous increase of the
334 bacterial burden in B6, followed by their death. The more abundant hematopoiesis and circulating
335 blood cells observed in SEG on D4, as well as their capacity to trap spleen bacteria within a
336 cellular reaction preventing massive destructive lesions, may thus reflect the results of the early
337 triggering of an efficient innate immune response in resistant animals rather than being the cause of
338 their recovery. Also arguing for the earliness of the response as being crucial for resistance is our
339 observation that the two mouse strains had the capacity to elicit the same effective G-CSF, KC,
340 MCP-1, IL-1 α and IL-6 responses when exposed to comparable bacterial loads. This would be
341 supported by the fact that, except for the IL-6R gene, no genetic determinant corresponding to
342 these five cytokines is located on the three mouse chromosomal loci recently shown by us to be
343 associated with SEG resistance to plague [18]. Thus, the major difference between B6 and SEG is
344 not the quality of their cytokine responses, but the time at which they are triggered.

345 In conclusion, comparison of the *Y. pestis* infection course and innate immune response in
346 susceptible and resistant mouse strains has shown that unexpectedly, the more efficient
347 colonization of SEG by *Y. pestis* early during the infectious process may be critical for the
348 triggering of an effective innate immune response.

349

350 **Funding**

351 This study was supported by a BIOTOX grant from the French Ministry of Health and a grant from
352 Aventis Pharma (Sanofi-Aventis group) and Bayer Pharma as part of a multi-organism call for
353 proposal. CB is a recipient of a DGA (*Délégation Générale pour l'Armement*) fellowship. The
354 Mouse functional Genetics Unit is supported by Merck Serono.

355

356 **Acknowledgements**

357 The authors wish to thank Professor J.L. Guénet for his support to the project and A. Ferreira for
358 help with flow cytometry.

359

360 **Conflict of Interest**

361 The authors have no conflicts of interest.

362

363 **References**

- 364 1. Perry RD, Fetherston JD. *Yersinia pestis*--etiologic agent of plague. Clin Microbiol Rev
365 **1997**; 10:35-66.
- 366 2. Inglesby TV, Dennis DT, Henderson DA, et al. Plague as a biological weapon - Medical and
367 public health management. J Am Med Assoc **2000**; 283:2281-90.
- 368 3. WHO. Human plague in 2002 and 2003. Wkly Epidemiol Rec **2004**; 79:301-8.
- 369 4. WHO. International meeting on preventing and controlling plague: the old calamity still has
370 a future. Wkly Epidemiol Rec **2006**; 81:278-84.
- 371 5. Guiyoule A, Gerbaud G, Buchrieser C, et al. Transferable plasmid-mediated resistance to
372 streptomycin in a clinical isolate of *Yersinia pestis*. Emerg Infect Dis **2001**; 7:43-8.
- 373 6. Galimand M, Guiyoule A, Gerbaud G, et al. Multidrug resistance in *Yersinia pestis* mediated
374 by a transferable plasmid. N Engl J Med **1997**; 337:677-80.

- 375 7. Guinet F, Ave P, Jones L, Huerre M, Carniel E. Defective innate cell response and lymph
376 node infiltration specify *Yersinia pestis* infection. PLoS One **2008**; 3:e1688.
- 377 8. Sebbane F, Gardner D, Long D, Gowen BB, Hinnebusch BJ. Kinetics of disease progression
378 and host response in a rat model of bubonic plague. Am J Pathol **2005**; 166:1427-39.
- 379 9. Thomas RE, Barnes AM, Quan TJ, Beard ML, Carter LG, Hopla CE. Susceptibility to
380 *Yersinia pestis* in the northern grasshopper mouse (*Onychomys leucogaster*). J Wildl Dis **1988**;
381 24:327-33.
- 382 10. Rahalison L, Ranjalahy M, Duplantier JM, et al. Susceptibility to plague of the rodents in
383 Antananarivo Madagascar. The Genus *Yersinia*. Vol. 529. New York: Kluwer
384 Academic/Plenum Publishers, **2003**. 439-442
- 385 11. Quan SF, Kartman L. Ecological studies of wild rodent plague in the San Francisco bay
386 area of California. VIII. Susceptibility of Wild Rodents to Experimental Plague Infection.
387 Zoonoses Research **1962**; 1:121-44.
- 388 12. Hubbert WT, Goldenberg MI. Natural resistance to plague: genetic basis in the vole
389 (*Microtus californicus*). Am J Trop Med Hyg **1970**; 19:1015-9.
- 390 13. Russel P, Eley SM, Hibbs SE, Manchee RJ, Stagg AJ, Titball RW. A comparison of Plague
391 vaccine, USP and EV76 vaccine induced protection against *Yersinia pestis* in a murine model.
392 Vaccine **1995**; 13:1551-6.
- 393 14. Philipovskiy AV, Cowan C, Wulff-Strobel CR, et al. Antibody against V antigen prevents
394 Yop-dependent growth of *Yersinia pestis*. Infect Immun **2005**; 73:1532-42.
- 395 15. Turner JK, McAllister MM, Xu JL, Tapping RI. The resistance of BALB/cJ mice to
396 *Yersinia pestis* maps to the major histocompatibility complex of chromosome 17. Infect Immun
397 **2008**; 76:4092-9.
- 398 16. Turner JK, Xu JL, Tapping RI. Substrains of 129 Mice Are Resistant to *Yersinia pestis*
399 KIM5: Implications for Interleukin-10-Deficient Mice. Infect Immun **2009**; 77:367-73.

- 400 17. Congleton YH, Wulff CR, Kerschen EJ, Straley SC. Mice naturally resistant to *Yersinia*
401 *pestis* Delta pgm strains commonly used in pathogenicity studies. *Infect Immun* **2006**;
402 74:6501-4.
- 403 18. Blanchet C, Jaubert J, Carniel E, et al. *Mus spretus* SEG/Pas mice resist virulent *Yersinia*
404 *pestis*, under multigenic control. *Genes Immun* **2011**; 12:23-30.
- 405 19. Guenet JL, Bonhomme F. Wild mice: an ever-increasing contribution to a popular
406 mammalian model. *Trends Genet* **2003**; 19:24-31.
- 407 20. Mishell B, Shiigi S. *Selected Methods in Cellular Immunology*. San Francisco: W.H.
408 Freeman and Co, **1980**.
- 409 21. Serbina NV, Pamer EG. Monocyte emigration from bone marrow during bacterial infection
410 requires signals mediated by chemokine receptor CCR2. *Nat Immunol* **2006**; 7:311-7.
- 411 22. Deshmane SL, Kremlev S, Amini S, Sawaya BE. Monocyte chemoattractant protein-1
412 (MCP-1): an overview. *J Interferon Cytokine Res* **2009**; 29:313-26.
- 413 23. Semerad CL, Liu F, Gregory AD, Stumpf K, Link DC. G-CSF is an essential regulator of
414 neutrophil trafficking from the bone marrow to the blood. *Immunity* **2002**; 17:413-23.
- 415 24. Walker F, Zhang HH, Matthews V, et al. IL6/sIL6R complex contributes to emergency
416 granulopoietic responses in G-CSF- and GM-CSF-deficient mice. *Blood* **2008**; 111:3978-85.
- 417 25. Maianski NA, Mul FP, van Buul JD, Roos D, Kuijpers TW. Granulocyte colony-
418 stimulating factor inhibits the mitochondria-dependent activation of caspase-3 in neutrophils.
419 *Blood* **2002**; 99:672-9.
- 420 26. Ozaki Y, Ohashi T, Kume S. Potentiation of neutrophil function by recombinant DNA-
421 produced interleukin 1a. *J Leukoc Biol* **1987**; 42:621-7.
- 422 27. Lira SA, Zalamea P, Heinrich JN, et al. Expression of the chemokine N51/KC in the
423 thymus and epidermis of transgenic mice results in marked infiltration of a single class of
424 inflammatory cells. *J Exp Med* **1994**; 180:2039-48.
- 425 28. Segal AW. How neutrophils kill microbes. *Annu Rev Immunol* **2005**; 23:197-223.

- 426 29. Serbina NV, Salazar-Mather TP, Biron CA, Kuziel WA, Pamer EG. TNF/iNOS-producing
427 dendritic cells mediate innate immune defense against bacterial infection. *Immunity* **2003**;
428 19:59-70.
- 429 30. Goodyear A, Jones A, Troyer R, Bielefeldt-Ohmann H, Dow S. Critical Protective Role for
430 MCP-1 in Pneumonic *Burkholderia mallei* Infection. *J Immunol* **2009**. 1445-54.
- 431 31. Adams DO, Hamilton TA. The cell biology of macrophage activation. *Annu Rev Immunol*
432 **1984**; 2:283-318.
- 433
- 434
- 435

436 **LEGEND TO FIGURES**

437

438 **Figure 1: Bacterial loads at different time points in the blood and organs of *Y. pestis*-infected**
439 **B6 and SEG.** Mice were infected sc with 100 cfu of CO92 and groups of 10 animals (combined
440 results of two independent experiments) were sacrificed on D1 to D4 pi. The bacterial loads in the
441 blood (cfu/ml), lymph nodes (cfu/2 lymph nodes), spleen, liver and lungs (cfu/g of tissue) were
442 determined for each animal and at each time point. Shown are means \pm s.e.m. of 9-10 mice per
443 point. Statistical differences between the two mouse strains at each time point were evaluated using
444 the Mann-Whitney-Wilcoxon rank sum test and are indicated by stars. *: $p < 0.05$; **: $p < 0.01$.

445

446 **Figure 2: Blood (A) and bone marrow (B) cell numbers during the course of infection in SEG**
447 **and B6.** Shown are the means \pm s.e.m. for 9-10 mice mice (blood) or 5 mice (bone marrow) at each
448 time point. Statistical differences between the two mouse strains at each time point were evaluated
449 using the Mann-Whitney-Wilcoxon rank sum test. *: $p < 0.05$, **: $p < 0.01$, ***: $p < 0.001$.

450

451 **Figure 3: Tissue lesions and cell populations in the spleen of infected SEG and B6.**
452 (A) Number of animals with histological lesions (positive mice/total) in the spleen. Scores (means
453 \pm s.e.m.) of hemorrhages (histological scale 0 to 3) and PMN infiltration (scale 0 to 5) and
454 summarize the observation of ≥ 60 microscopic fields (≥ 20 fields/section with a X20 objective on
455 ≥ 3 complete sections per sample). (B) Hematoxylin-Eosin (a, b) and anti-F1 immunohistochemical
456 staining (c, d) of spleen sections taken on D4 pi. B6 spleens had abundant foci of necrosis (small
457 arrows in a) containing numerous bacteria (red-brown color in c), while SEG spleens exhibited
458 some micro abscesses (large arrowhead in b) without necrosis and containing few bacteria (d). The
459 2-tailed non-parametric Mann-Whitney-Wilcoxon rank sum test was used to compare groups. *:
460 $p \leq 0.05$, **: $p \leq 0.01$. (C) Quantification of different spleen cell populations in B6 and SEG (12
461 animals each from two independent experiments, except for T cells where 7 animals were

462 analyzed). Splenocytes were counted microscopically and macrophages (MP), polymorphonuclear
463 neutrophils (PMN) and T cells were quantified by flow cytometry. Individual results from
464 uninfected (0, white diamonds) or infected (D2 pi, grey circles) animals are plotted. "+" on each
465 side of the columns indicate mean values. The 2-tailed non-parametric Mann-Whitney-Wilcoxon
466 rank sum test was used to compare groups. *: $p \leq 0.05$, **: $p \leq 0.01$, ***: $p \leq 0.001$.

467

468 **Figure 4: Cytokine contents in the plasma, spleen and inguinal lymph nodes of B6 and SEG**
469 **during the course of a *Y. pestis* infection.** Shown are the values for five cytokines (G-CSF, KC,
470 MCP-1, IL-1 α and IL-6) in individual SEG (grey rectangles) and B6 (grey triangles) mice from D0
471 to D4 pi for 10 animals (9 for B6 on D4), and the median curves (plain lines for B6, and dotted
472 lines for SEG). Groups were compared using the non-parametric Mann-Whitney-Wilcoxon rank
473 sum test. *: $p \leq 0.05$; **: $p \leq 0.01$; ***: $p \leq 0.001$. Stars above the comparison bar indicate values
474 significantly superior in SEG, while stars below the comparison bar indicate values significantly
475 superior in B6.

476

Table 1. Correlation between bacterial load and cytokine content in tissues of infected mice

		SEG			B6		
		Plasma	Spleen	LN	Plasma	Spleen	LN
G-CSF	r:	0.50	0.67	0.45	0.69	0.68	0.57
	p:	0.0005	<0.0001	0.002	<0.0001	<0.0001	<0.0001
IL-1α	r:	0.41	0.57	0.39	0.57	0.55	0.50
	p:	0.005	<0.0001	0.009	<0.0001	0.0001	0.0005
IL-6	r:	0.52	0.54	nss	0.70	nss	0.54
	p:	0.0002	0.0001		<0.0001		0.0001
KC	r:	0.51	0.75	0.57	0.59	0.84	0.64
	p:	0.0003	<0.0001	<0.0001	<0.0001	<0.0001	<0.0001
MCP-1	r:	0.62	0.54	nss	0.71	0.42	0.45
	p:	<0.0001	0.0001		<0.0001	0.005	0.002
IL-1β	r:	nss	0.57	nss	nss	0.52	0.44
	p:		<0.0001			0.0003	0.003
IL-10	r:	nss	nss	nss	nss	nss	nss
	p:						
TNFα	r:	0.41	nss	nss	0.54	nss	nss
	p:	0.005			0.0002		
IFNγ	r:	nss	nss	nss	nss	nss	nss
	p:						
IL-12p70	r:	0.53	nss	nss	nss	nss	nss
	p:	0.0002					

NOTE: The non parametric Spearman rank test (r) was used to evaluate the correlation between cfu values and the level of each cytokine, regardless of the time pi. To account for multiple testing, a Bonferroni correction was applied so only correlation values with $p < 0.01$ were retained, and in such cases both p and r values are given. Non statistically significant values were noted as nss. SEG samples: n=40, B6 samples: n=39. LN: lymph nodes.

Figure 1

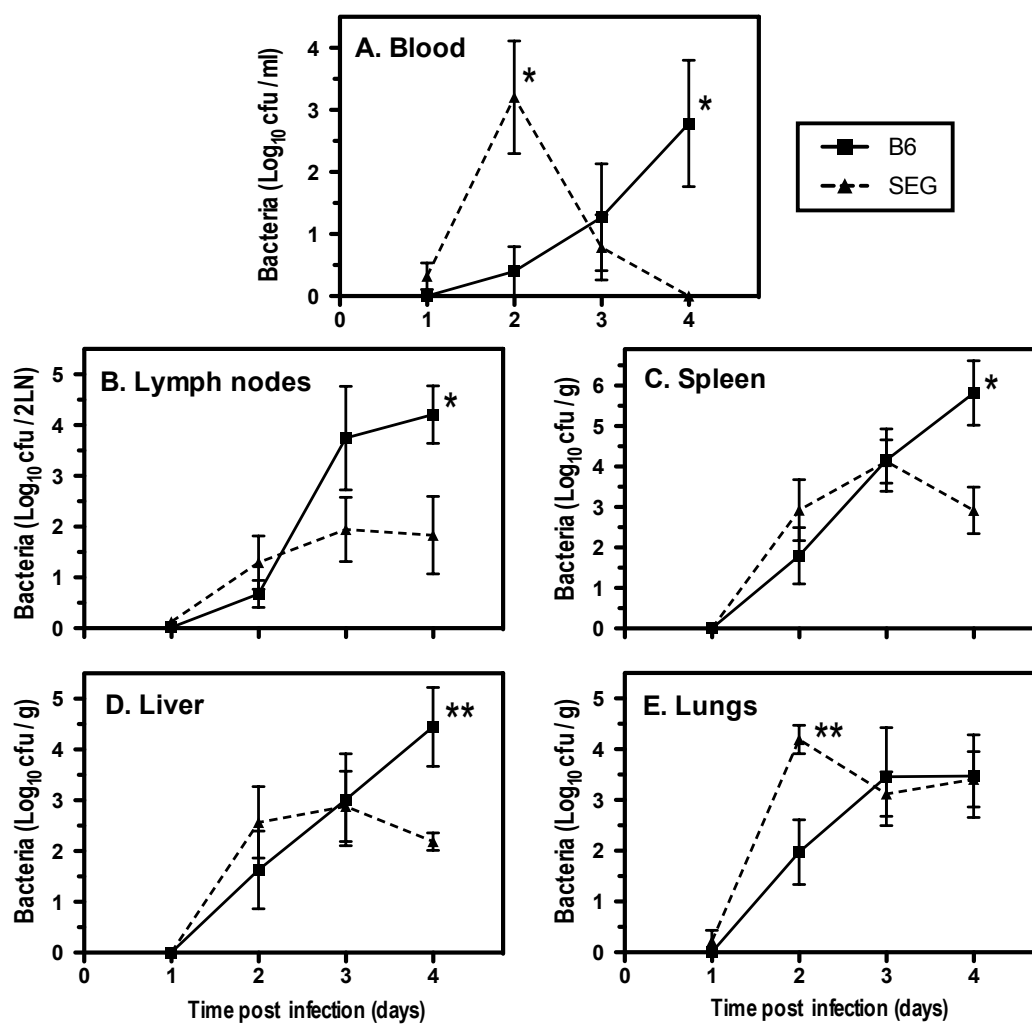
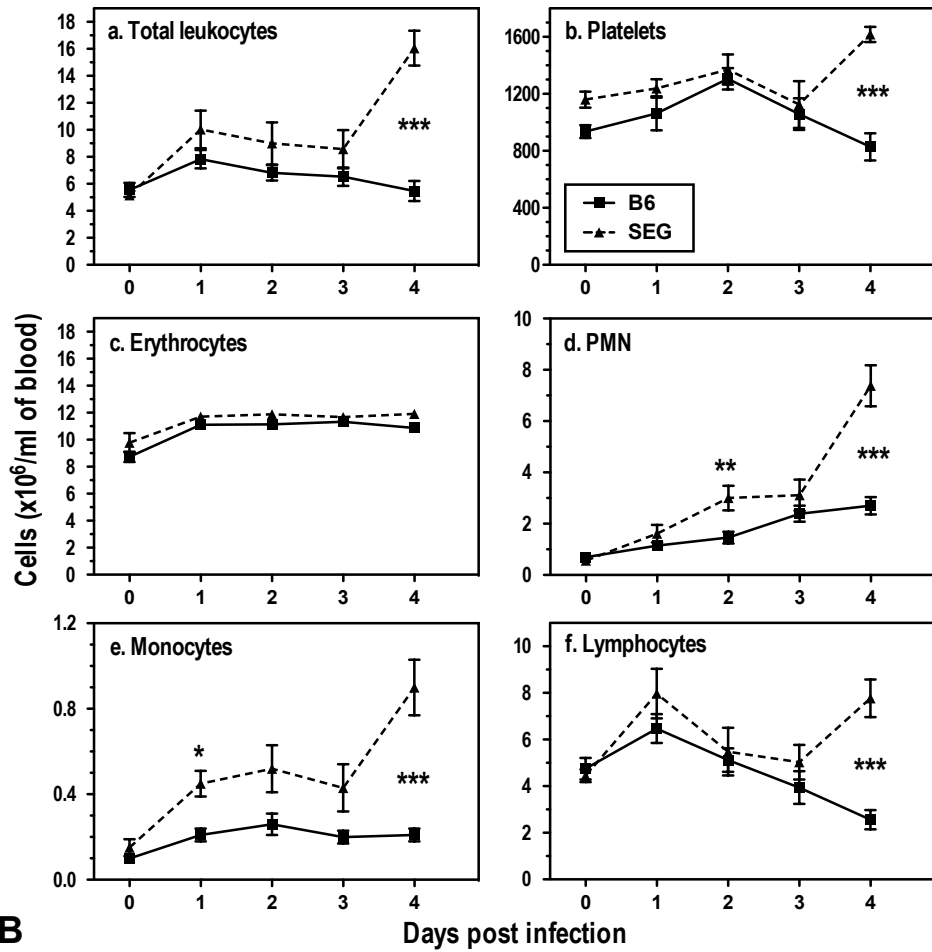


Figure 2

A



B

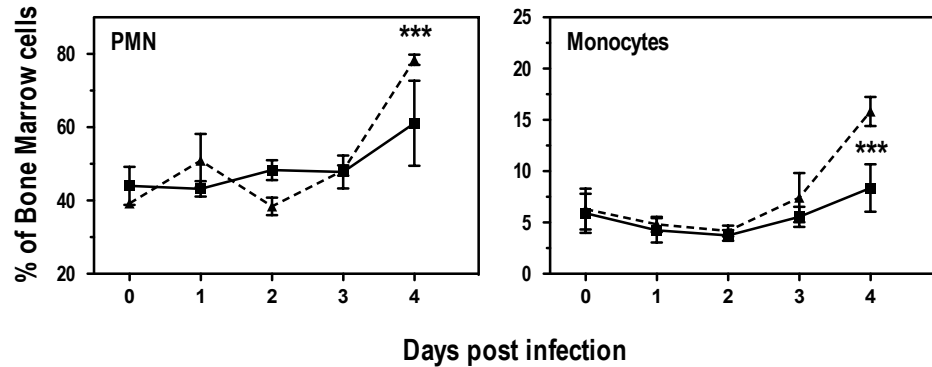
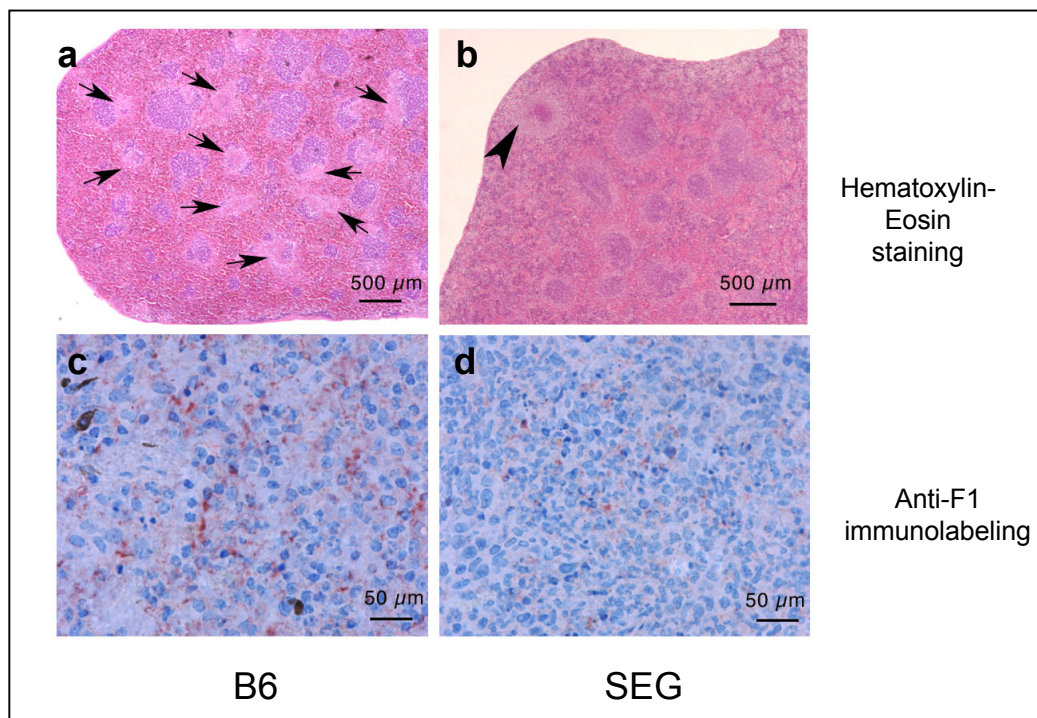


Figure 3

A

	Day 1		Day 2		Day 3		Day 4	
	B6	SEG	B6	SEG	B6	SEG	B6	SEG
Mean score								
Hemorrhages	0	0	0.6 (±0.1) *	0.2 (±0.1)	1.0 (±0.1) **	0.3 (±0.1)	1.0 (±0.2)	0.4 (±0.2)
PMN infiltrates	0.3 (±0.1)	0.3 (±0.1)	0.6 (±0.1)	0.5 (±0.1)	1.3 (±0.2) *	0.9 (±0.1)	1.9 (±0.5)	1.3 (±0.2)
Nb of mice affected/total								
Congestion	1/10	1/10	0/10	0/10	2/10	4/10	3/9	2/10
Necrosis	0/10	0/10	0/10	0/10	0/10	0/10	3/9	0/10
Micro abscesses	0/10	0/10	0/10	0/10	1/10	1/10	0/9	3/10

B



C

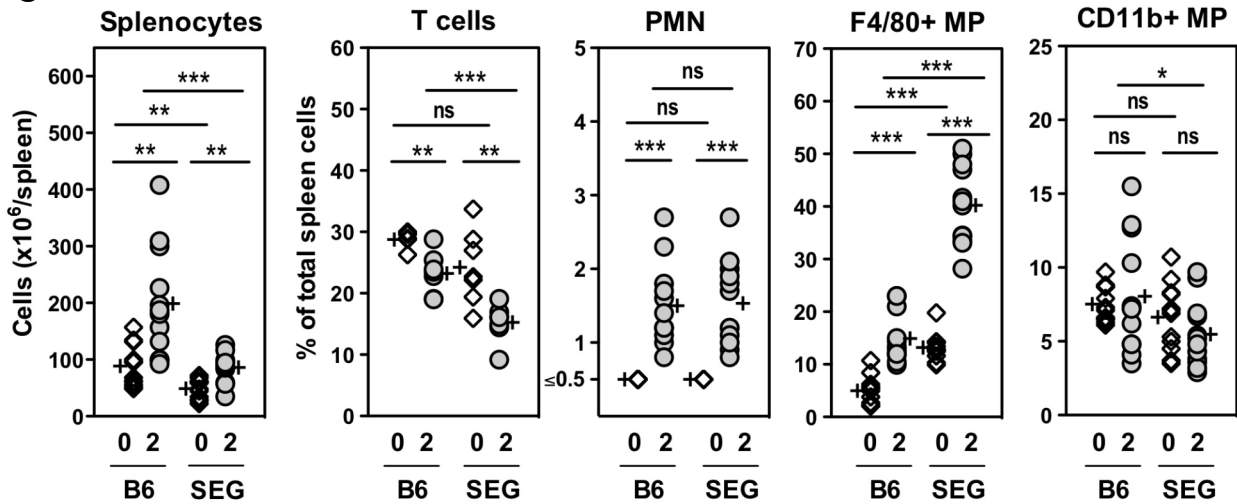
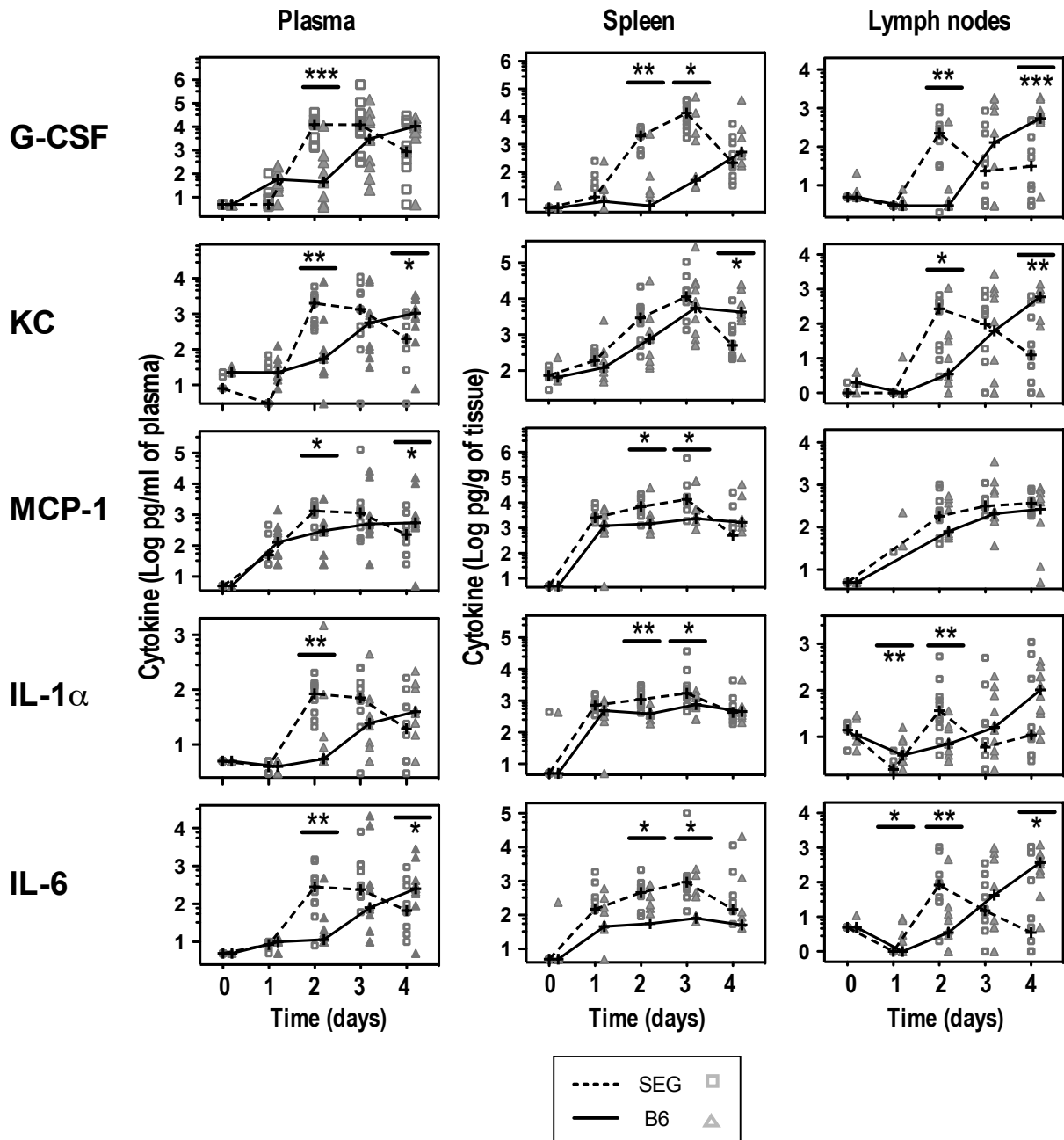
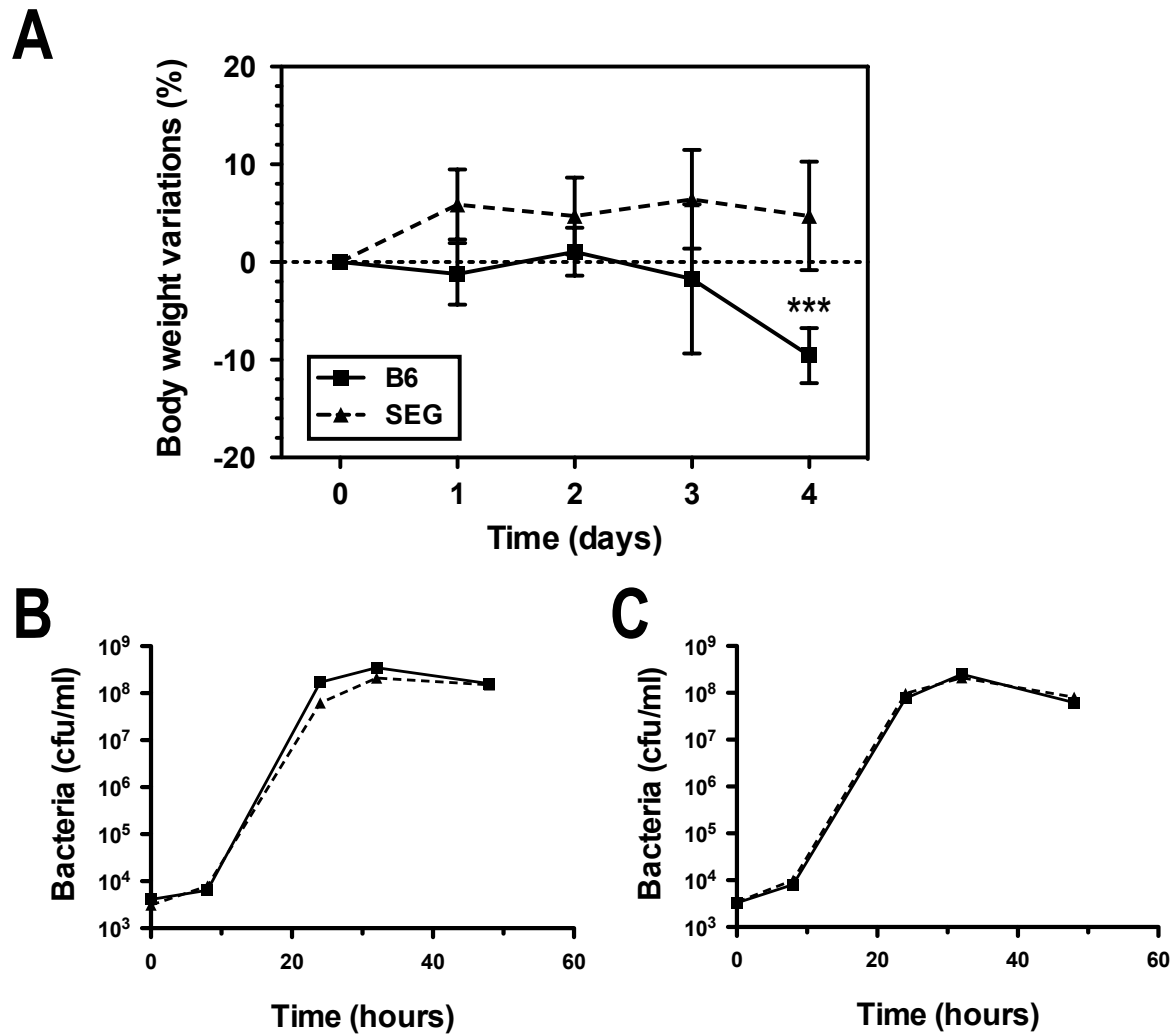


Figure 4

[Click here to download Figure: C_Demeure_2011_Fig.4_JID2.pdf](#)

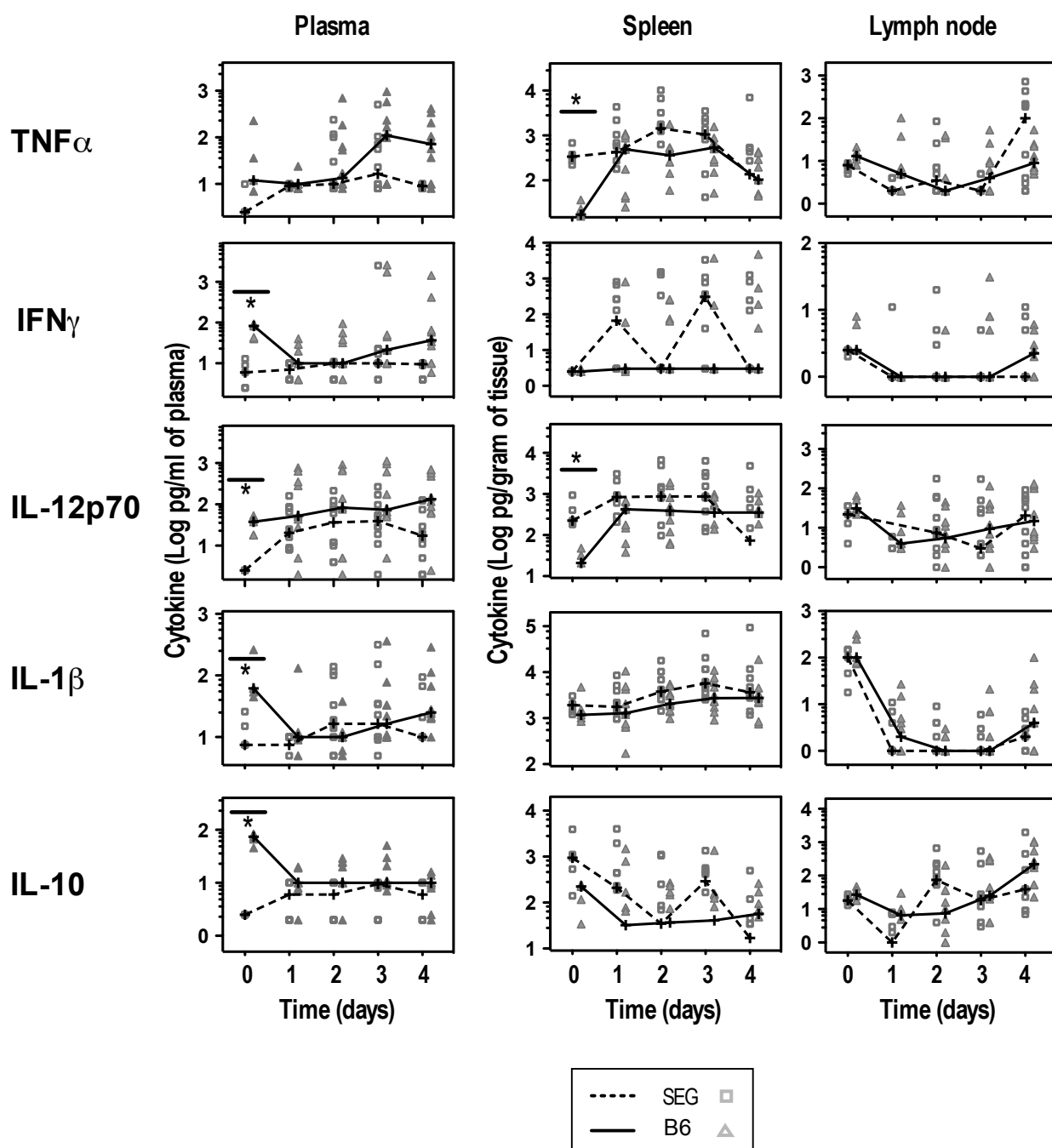
Figure 4





Supplementary figure S1: Comparison of B6 and SEG mice for body weight variations during infection and growth of *Y. pestis* in their serum

The weight of each animal was recorded daily after infection (A) and variation was calculated using the weight at day 0 as a reference. Shown are means \pm sem of 9-10 mice per time point and per mouse strain. Stars indicate significant differences between the two mouse strains at a given time point determined using the Mann-Whitney-Wilcoxon rank sum test. ***: $p < 0.001$. To determine the contribution of serum to the control of bacteremia by SEG mice, pools of undecomplemented sera collected from SEG or B6 mice prior to infection (B), or two days post infection (C) were inoculated with 10^3 cfu/ml of *Y. pestis* CO92 and incubated at 37°C . Serum aliquots were taken at different time points for bacterial count determination.



Supplementary Figure S2: Cytokine contents in the plasma, inguinal lymph nodes and spleen of B6 and SEG during the course of a *Y. pestis* infection.

Shown are the values for TNF α , IFN γ , IL-12p70, IL-1 β , and IL-10 in 10 individual SEG (grey rectangles) or B6 (grey triangles, 9 animals for B6 on D4) mice from D0 to D4 pi, and the median curves (plain lines for B6, and dotted lines for SEG). The Wilcoxon statistical test was used to compare groups. *: $p \leq 0.05$. Stars above the comparison bar indicate values significantly superior in SEG, while stars below the comparison bar indicate values significantly superior in B6.